Alkyl Propoxy Ethoxylate "Graded" Surfactants: Micelle Formation and Structure in Aqueous Solutions

Biswajit Sarkar and Paschalis Alexandridis*

Department of Chemical and Biological Engineering, University at Buffalo, The State University of New York (SUNY), Buffalo, New York 14260-4200

Received: November 17, 2009; Revised Manuscript Received: January 26, 2010

The self-assembly of alkyl propoxy ethoxylate surfactants in aqueous solutions has been investigated with a focus on the (i) thermodynamics of micellization (critical micellization concentration; free energy, enthalpy, and entropy of micellization) and (ii) structure of the micelles (overall shape and size; local environment in the micelle core and corona) as affected by the surfactant composition (variation of degree of ethoxylation). The various results are compared to those for alkyl ethoxylate and poly(ethylene oxide)-*b*-poly(propylene oxide) amphiphiles with the aim to elucidate the role of the middle, propoxy, block in the novel alkyl propoxy ethoxylate surfactants which exhibit a "graded" hydrophobic−hydrophilic character.

Introduction

Alkyl ethoxylates (C_iEO_j) are nonionic surfactants that exhibit low critical micellization concentrations (cmc), compatibility with other surfactants, and mild nature. These surfactants are widely used in personal care products, detergency, paint formulation, controlled drug delivery, etc.[1−3] Considering its broad, fundamental, and technical applicability, the micellization of these surfactants in aqueous solution has been extensively investigated, both experimentally[4−10] and theoretically.[11−14] The following trends have emerged for C_iEO_j nonionic surfactants in aqueous solution: the log(cmc) decreases linearly with alkyl chain length;[9] the influence of alkyl chain on the cmc becomes smaller at higher temperature;[15] the cmc increases as the poly(ethylene oxide) (PEO) block length increases; and the cmc decreases as the temperature increases.[10,16] The structure of micelles formed by C_iEO_j surfactants in water has been probed using small-angle X-ray and neutron scattering.[17−20] An ellipsoidal core shell form factor was used to describe the $C_{12}EO_{32}$ (Brij 35) micelles and the micelle association number was found to increase with surfactant concentration.[17] The micelles formed by $C_{18}EO_{100}$ (Brij 700) surfactants were described with a spherical core shell model.[21] The formation of C_iEO_j micelles in aqueous solution is driven by the "hydrophobic effect" which originates from more favorable water−water interactions over less favorable interactions between alkyl chains and water molecules.[22,23] During the assembly of the alkyl chains in the micelle core, the hydrophilic poly(ethylene oxide) head groups are placed at the alkyl−water interface. As the headgroup size increases, the steric repulsion between PEO blocks also increases, which disfavors micellization.

Alkyl propoxy ethoxylates ($C_iPO_nEO_j$) are a novel class of nonionic surfactants which, among other applications, have been recently used successfully in nanomaterial synthesis.[24] The middle poly(propylene oxide) (PPO) block possesses a hydrophobicity/hydrophilicity intermediate to that of the alkyl and PEO blocks. Thus, the $C_iPO_nEO_j$ surfactants can be described as having gradient hydrophobic/hydrophilic properties. In the case of the well-studied $EO_jPO_nEO_j$ (Pluronic) triblock copolymers, PPO has a definite hydrophobic character.[25−30] However, the role that PPO plays in the $C_iPO_nEO_j$ surfactants is not clear.

The difference in the interaction of water with PEO and PPO can be interpreted in terms of the water structural model proposed by Kjellander and Florin.[31] According to this model, PEO can fit very well in the tetrahedral water structure, and even enhances the water structure. On the other hand, PPO has a methyl group which confers steric hindrance. Therefore, PPO does not fit well in the water structure and hence it behaves as less hydrophilic compared to PEO.

Recently, our group investigated the phase behavior and structure of $C_iPO_nEO_j$ surfactants at high concentrations in aqueous solutions using a mean-field lattice model.[32,33] We found a thermotropic phase behavior to dominate over the lyotropic behavior, and several ordered phases to be stable at room temperature. This domination of the thermotropic phase transitions over the lyotropic was explained on the basis of a rapid decrease in solvent quality for both PEO and PPO segments at elevated temperature, and a decrease in incompatibility between alkyl and PEO segments. No literature data on the aqueous solution behavior of $C_iPO_nEO_j$ surfactants at low concentrations have been reported yet, hence we pursued the study presented here. In particular, we measured the cmc values of three $C_iPO_nEO_j$ surfactants (with varying degree of ethoxylation) in aqueous solution using UV−vis and fluorescence spectroscopy, and probed the micelle structure with small-angle X-ray scattering (SAXS). We organize the results and discussion in two parts: in the first part we examine the thermodynamics of micellization in water and use such information to determine the role of poly(propylene oxide) in the $C_iPO_nEO_j$ micellization. In the second part, we present various micelle structural parameters, such as radius, association number, and solvation. In both parts we compare the self-assembly properties of $C_iPO_nEO_j$ to those of the better-studied C_iEO_j and $EO_jPO_nEO_j$ amphiphiles. To the best of our knowledge, this is the first report of micellization of alkyl propoxy ethoxylate surfactants in aqueous solution.

Materials

Surfactants. Three surfactants with the chemical structure alkyl propoxy ethoxylate ($C_iPO_nEO_j$) and varying length of EO

* To whom correspondence should be addressed. E-mail: palexand@buffalo.edu.

10.1021/jp910939q
Published on Web 03/11/2010

TABLE 1: Composition of Surfactants Used in This Study

amphiphile	mol struct	mol wt	EO content (wt %)	alkyl/EO ratio (wt/wt)	PO/EO ratio (wt/wt)
S1	$C_{13}(PO)_{12.2}(EO)_8$	1266	30	0.49	1.94
S2	$C_{13}(PO)_{12.2}(EO)_{17}$	1641	46	0.24	0.91
S3	$C_{13}(PO)_{12.2}(EO)_{34}$	2390	63	0.12	0.46

segment were obtained from Dow Chemical Co., Midland, MI, and were used as received. Their nominal compositions are shown in Table 1. These three surfactants can also be considered as short chain ABC triblock terpolymers with hydrophobic poly(ethylene) and hydrophilic poly(ethylene oxide) (PEO) blocks at the two ends, and poly(propylene oxide) (PPO) block at the middle.[34,35]

Spectroscopic Probes. 1,6-Diphenyl-1,3,5-hexatriene (DPH) (obtained from Sigma, St. Louis, MO) was used to determine the critical micellization concentration (cmc) of the surfactants in water. Pyrene (Fluka, Switzerland) was used to probe the cmc and the micropolarity of the surfactant solution. Both were used as received.

Sample Preparation. Stock solutions of surfactants were prepared by dissolving them in Milli-Q water. Samples were prepared by diluting the stock solutions to the desired surfactant concentration (in the concentration ranges of 0.0001−0.25 wt % for surfactant S1 and 0.0001−1 wt % for S2 and S3; see Table 1 for surfactant notation). The solubility of S1 (having the shortest PEO chain) in water was rather low and the solution became turbid above 0.3 wt %. The solutions were tested within a few days of preparation.

DPH Addition. A stock solution of 0.7 mM DPH in methanol was prepared: 25 μL of the DPH/methanol solution was added to 3 g of surfactant solution, so that the final solution contained less than 0.004 mM DPH and 1% v/v methanol.[29] The same DPH concentration (0.004 mM) was used for all samples. The solutions were left in the dark to equilibrate for at least 3 h (and no more than 24 h) before the spectroscopic measurement.

Pyrene Addition. A stock solution of 1 mM pyrene in ethanol was prepared, which was further diluted to 1 μM. Two microliters of the 1 μM pyrene/ethanol solution was added to 3 g of surfactant solution. The resulting pyrene and ethanol concentrations were about 0.006 μM and 0.067 vol %, respectively.

Methods

UV−Vis Spectroscopy. Absorption spectra of the DPH-containing surfactant solutions (placed in Teflon-stoppered quartz cuvettes) were recorded in the 300−500 nm range at 25 and 40 °C using a Hitachi U-1800 UV−vis spectrophotometer. The absorption intensity is a function of the concentration of solubilized DPH. At surfactant concentrations below the cmc, DPH was not solubilized in a hydrophobic environment and the UV−vis absorption intensity due to DPH was very low. When micelles formed, DPH was solubilized in the hydrophobic micelle core resulting in a characteristic spectrum with the main peak at 356 nm.[29] The absorption intensity at 356 nm has been plotted vs the logarithm of surfactant concentration, and the cmc values were determined from the first inflection point of this curve (these graphs are not presented here).

Fluorescence Spectroscopy. The fluorescence emission intensity of pyrene-containing aqueous surfactant solutions (at an excitation wavelength of $\lambda = 335$ nm) was recorded in the 350−600 nm range using a Hitachi 2500 fluorescence spectrophotometer. Five vibronic peaks characteristic of pyrene were observed. The ratio of the first to the third vibronic peak (I_1/I_3) decreases with decreasing polarity of the pyrene microenvironment.[36] As the surfactant concentration increased toward the cmc, pyrene started to partition to hydrophobic sites and, as a result, the I_1/I_3 ratio started to decrease. At concentrations well above cmc, pyrene had accumulated into hydrophobic moieties and the I_1/I_3 ratio value stabilized. The I_1/I_3 ratios for aqueous solutions of S1, S2, and S3 have been plotted against the logarithm of surfactant concentrations (graphs not presented here) and the cmc values were determined from the second inflection of this curve.[37] The cmc values obtained from pyrene fluorescence compared well with those obtained from DPH absorption.

Small-Angle X-ray Scattering (SAXS). The SAXS technique was applied to examine the micellar structure of S2 and S3 surfactants in aqueous solutions (due to its relatively low solubility in water, the S1 concentration at which we collected SAXS data gave rather low signal-to-noise ratio that did not allow for unambiguous data analysis). The SAXS experiments were performed using a Nano-STAR instrument (Bruker-AXS, Madison, WI) operated at 40 kV and 35 mA. The surfactant solutions were tested at 25 °C in a quartz capillary with an outer diameter of 2 mm. The sample to detector distance was 1015 mm. The X-ray wavelength (λ) used was 0.1542 nm (Cu Kα). The angular distribution of the scattered electrons was recorded in a two-dimensional detector. The scattering intensity was obtained by averaging the intensity of all points in the 2-D detector space for a scattering vector value, q, defined as

$$q = \frac{4\pi}{\lambda}\sin(\Theta/2) \tag{1}$$

Θ is the angle between the incident beam and the scattered radiation.

The reduction of data to absolute scale was carried out following procedures described in ref 38. Scattering from water was used as background. Transmission measurements were done indirectly by measuring the scattering from glassy carbon with and without sample. Noise correction was made using eq 2.[38]

$$T = (I_{GC+S} - T_{GC}I_S)/I_{GC} \tag{2}$$

where T is the corrected transmission of the sample, I_{GC} the noise-subtracted integrated number of counts for glassy carbon, I_{GC+S} the count number from glassy carbon with sample, T_{GC} the transmission from glassy carbon, and I_S the noise-subtracted number of counts for the sample. Data obtained from pixels close to the beam stop were corrected using a first-order correction procedure.[38]

SAXS Data Evaluation. The SAXS scattering intensity originating from a system of particles can be written as[39]

$$I(q) = n_P P(q) S(q) \tag{3}$$

where n_p is the particle number density, $P(q)$ the particle form factor (that captures the structure of the micelle), and $S(q)$ the particle structure factor (accounts for intermicellar interactions).

A core−shell ellipsoid form factor (eq 4)[40] has been used here to describe the micelle internal structure (see Results and Discussion for model selection). The core containing alkyl chains is assumed to be solvent free, whereas the shell is highly

solvated. The scattering results from the differences in electron density between core and shell, and between shell and bulk solvent.

$$P(q) = \frac{\text{Scale}}{V_{\text{shell}}} \int_0^1 |F(q, r_i, \alpha)|^2 \, d\alpha + \text{bkg} \quad (4)$$

For oblate (disk shape) core shell ellipsoids, $F(q,r_i,\alpha)$ in eq 4 is expressed as[40,41]

$$F_{\text{oblate}}(q, r_i,\alpha) = \frac{3(\rho_{\text{core}} - \rho_{\text{shell}})V_{\text{core}} j_1(u_{\text{core}})}{u_{\text{core}}} + \frac{3(\rho_{\text{shell}} - \rho_{\text{solvent}})V_{\text{shell}} j_1(u_{\text{shell}})}{u_{\text{shell}}} \quad (5)$$

where

$$V_{\text{core}} = \frac{4\pi}{3} r_{\text{min/core}} r_{\text{maj/core}}^2 \quad (6)$$

$$V_{\text{shell}} = \frac{4\pi}{3} r_{\text{min/shell}} r_{\text{maj/shell}}^2 \quad (7)$$

$$u_{\text{core}} = q[r_{\text{maj/core}}^2(1 - \alpha^2) + r_{\text{min/core}}^2\alpha^2]^{1/2} \quad (8)$$

$$u_{\text{shell}} = q[r_{\text{maj/shell}}^2(1-\alpha^2) + r_{\text{min/shell}}^2\alpha^2]^{1/2} \quad (9)$$

$$j_1(x) = (\sin x - x \cos x)/x^2 \quad (10)$$

Here ρ is the scattering length density, V_{core} is the volume of the micelle core, $r_{\text{min,core}}$ is the micelle minor core radius, $r_{\text{maj,core}}$ is the micelle major core radius, V_{shell} is the volume of the whole micelle, $r_{\text{min,shell}}$ is the micelle minor radius, $r_{\text{maj,shell}}$ is the micelle major radius, Scale is a free fitting parameter, and bkg is a free fitting parameter that accounts for incoherent scattering.

Intermicellar interactions are accounted through the hard-sphere structure factor $S(q)$.[42]

$$S(q) = 1/[1 + 24\Phi G(2qr_{\text{HS}})/(2qr_{\text{HS}})] \quad (11)$$

Φ is the micellar volume fraction, r_{HS} is the hard-sphere interaction radius, and G is a trigonometric function of $A = 2qr_{\text{HS}}$ and Φ.

$$G(A, \Phi) = \frac{\alpha(\sin A - A \cos A)}{A^2} + \frac{\beta[2A \sin A + (2 - A^2)\cos A]}{A^2} + \gamma\{-A^4 \cos A + 4[(3A^2 - 6)\cos A + (A^3 - 6)\sin A + 6]\}/A^5 \quad (12)$$

where α, β, and γ are

$$\alpha = (1 + 2\Phi)^2/(1 - \Phi)^4$$

$$\beta = -6\Phi(1 + \Phi/2)^2/(1 - \Phi)^4$$

$$\gamma = (\Phi/2)(1 + 2\Phi)^2/(1 - \Phi)^4$$

The degree of solvation (i.e., water present in the micelle shell) can be calculated from the total volume of the shell and the volume occupied by PEO and PPO, by considering the micelle major shell radius to be the outer boundary of the hydrophilic domains, and the minor core radius to be the inner boundary. The volume fraction of water present in the micelle shell ($\Phi_{\text{solvation}}$) can be estimated as

$$\Phi_{\text{solvation}} = \frac{\left[\left(\frac{4\pi r_{\text{majshell}}^3}{3} - V_{\text{core}}\right) - V_{\text{PEO+PPO}}\right]}{\left(\frac{4\pi r_{\text{majshell}}^3}{3} - V_{\text{core}}\right)} \quad (13)$$

The degree of solvation can also be described as the average number of water molecules per EO or PO segment ($N_{\text{solvation,EO/PO}}$):

$$N_{\text{solvation,EO/PO}} = \frac{(V_{\text{shell}} - V_{\text{PEO+PPO}}) \,/\, v_{\text{water}}}{(j + n)N_{\text{association}}} \quad (14)$$

where $V_{\text{PEO+PPO}}$ is the total volume of PEO and PPO blocks in the micelle, v_{water} is the molecular volume of water which is calculated considering its density of 1 g/mL, and $N_{\text{association}}$ is the micelle association number, i.e., the average number of surfactant molecules in one micelle. The micelle association number is calculated as $N_{\text{association}} = V_{\text{core}}/V_{\text{alkyl chain}}$ (the volume of the C_{13} alkyl chain is 350.3 Å^3).

Results and Discussion

Micelle Formation. The cmc values extracted from DPH absorption and pyrene fluorescence data at 25 and 40 °C are presented in Table 2. As the surfactant PEO block length increased the cmc also increased. With an increase in temperature the cmc decreased for all three surfactants. In what follows, we analyze these data to discuss the role that the different parts of the $C_iPO_nEO_j$ surfactants play on micellization.

Thermodynamics of Micellization. The micellization of nonionic surfactants can be described with the closed association model which assumes an equilibrium between individually dissolved surfactant molecules and micelles.[29] According to this model, the change in the standard free energy ($\Delta G°$) for transfer of one mole of surfactant molecules from an aqueous solution to the micellar phase is given by[29]

$$\Delta G° = RT \ln(X_{\text{cmc}}) \quad (15)$$

where R is the ideal gas constant, T the absolute temperature, and X_{cmc} the surfactant mole fraction at the critical micellization concentration.

The standard enthalpy of micellization ($\Delta H°$) (assumed independent of temperature for the temperature range considered) can be obtained through the following equation:

$$\Delta H_{\text{mic}}° = -RT^2\left(\frac{\partial \ln X_{\text{mic}}}{\partial T}\right) \quad (16)$$

TABLE 2: Critical Micellization Concentration for S1, S2, and S3 in Aqueous Solutions

	cmc at					
surfactant	25 °C (wt %)	40 °C (wt %)	25 °C (mol/L)	40 °C (mol/L)	25 °C (mole fraction)	40 °C (mole fraction)
S1	0.01	0.008	7.90×10^{-5}	6.32×10^{-5}	1.42×10^{-6}	1.14×10^{-6}
S2	0.02	0.01	1.22×10^{-4}	6.09×10^{-5}	2.19×10^{-6}	1.10×10^{-6}
S3	0.05	0.02	2.09×10^{-4}	8.37×10^{-5}	3.77×10^{-6}	1.51×10^{-6}

TABLE 3: Free Energies ($\Delta G°$) of Micellization at Different Temperatures, and Standard Enthalpies ($\Delta H°$) and Entropies ($\Delta S°$) of Micellization for S1, S2, and S3 in Aqueous Solutions

surfactant	ΔG at 25 °C (kJ/mol)	ΔG at 40 °C (kJ/mol)	$\Delta H°$ (kJ/mol)	$\Delta S°$ (kJ/(mol K))
S1	−33.4	−33.9	11.0	0.15
S2	−32.3	−34.0	34.1	0.22
S3	−30.9	−33.2	45.1	0.26

The standard entropy of micellization ($\Delta S°$) can be calculated from the free energy and enthalpy:

$$\Delta S°_{mic} = (\Delta H°_{mic} - \Delta G°_{mic})/T \quad (17)$$

The micellization standard free energy $\Delta G°$, enthalpy $\Delta H°$, and entropy $\Delta S°$ values calculated from the experimental data according to the above equations are reported in Table 3. Negative values of $\Delta G°$ and positive values of $\Delta H°$ and $\Delta S°$ were obtained. The more negative $\Delta G°$ values at 40 °C reflect the fact that higher temperature favors micellization.

The positive enthalpies of micellization indicate that the transfer of a $C_iPO_nEO_j$ surfactant molecule from solution to a micelle is an enthalpically unfavorable, endothermic process. $\Delta H°$ values for S1, S2, and S3 are 11.0, 34.1, and 45.1 kJ/mol, respectively. The origin of positive $\Delta H°$ has been ascribed to the energy penalty associated with the hydrogen bond breaking during micellization.[29] As the number of EO units increases in the surfactant molecule, the number of hydrogen-bonding sites between surfactant and water increases, and thus $\Delta H°$ would increase.

The unfavorable enthalpy is overwhelmed by a favorable, positive entropy. $\Delta S°$ values for S1, S2, and S3 are 0.15, 0.22, and 0.26 kJ/(mol K), respectively. The positive $\Delta S°$ values can be viewed in the context of the very low solubility of hydrocarbons in water which is known as "hydrophobic effect".[22,23] A decrease of entropy is caused to water upon the introduction of hydrocarbon molecules. Micellization is related to the transfer of alkyl chains from aqueous solution to oil-like micelle cores, releasing water and hence increasing its entropy. The gain in the water entropy dominates over the loss in entropy due to the localization of hydrocarbon chains in the micelle core.[23,29] Hydration of PEO segments has been offered as an alternative (additional) explanation for the origin of positive $\Delta S°$ in the case of alkyl ethoxylate (C_iEO_j) surfactants.[22,43] An increase in $\Delta S°$ with the number of EO units was observed for C_iEO_j surfactants,[44] similarly to what is found for the $C_iPO_nEO_j$ surfactants of interest here.

Role of PPO in Self-Assembly. It is straightforward to calculate the free energy of micellization from eq 15 using experimentally determined cmc values. The free energy of micellization can be broken down into a number of contributions that depend on molecular interactions, e.g., (i) hydrophobic interaction, (ii) hydrophilic interaction or headgroup repulsion, (iii) contact between hydrocarbon and solvent, and (iv) packing.[45] Among those contributions, the free energy due to packing is typically found to be negligible. The hydrophobic free energy contribution is negative, while the headgroup interactions lead to the most significant positive contribution to $\Delta G°$.[45] Thus, the total free energy of micellization can be expressed in terms of two major contributions, ΔG(hydrophobic) and ΔG(hydrophilic). Such simplification allows us to break down the free energy of micellization according to the chemical structure of the surfactant molecule. In the present work, we are interested in extracting the free energy contribution due to PPO with an aim to establish the role of PPO in the self-assembly of $C_iPO_nEO_j$ surfactants in aqueous solution.

For the alkyl propoxy ethoxylate nonionic surfactants of interest here, the total free energy of micellization can be ascribed to three contributions (eq 18): (i) free energy due to transfer of alkyl chains from water to micelles, (ii) free energy due to PEO, and (iii) free energy due to PPO.

$$\Delta G° = \Delta G(C) + \Delta G(PO) + \Delta G(EO) \quad (18)$$

ΔG(C) can be estimated from the following empirical correlation (eq 19, where N_C is the number of carbon atoms present in the alkyl chain). The ΔG(C) value (in kJ/mol) thus calculated is reported in Table 4.[45]

$$\Delta G(C) = -3.0(N_C - 1) - 9.6 \quad (19)$$

We extracted the ΔG(EO) contribution starting from $\Delta G°$ values for a series of C_iEO_j surfactants (calculated from cmcs at 25 °C reported in the literature[46]) and subtracting ΔG(C) (calculated from eq 19). In order to represent the $C_iPO_nEO_j$ compositions of interest here, we extrapolated the ΔG(EO) dependence on EO for $N_{EO} = 34$, and interpolated for $N_{EO} = 17$ and $N_{EO} = 8$. These ΔG(EO) values are given in Table 4.

ΔG(PO) can now be calculated from eq 18. We found ΔG(PO) to be positive for the three $C_iPO_nEO_j$ surfactants at 25 °C (see Table 4), intimating that PPO is disfavoring micellization just like PEO. The same procedure can be used to estimate ΔG(PO) at 40 °C. It appears that ΔG(PO) becomes less positive at 40 °C; however, we do not report these ΔG(PO) values here, as data for micellization of C_iEO_j surfactants at 40 °C (needed for ΔG(EO) calculation) are less reliable.

Having established the hydrophilic role of PPO in the C_iEO_j micellization, we now compare the hydrophilicity of PPO to that of PEO. We found $\Delta G(PO)/N_{PO}$ to increase from 0.23 to 0.36 kJ/mol PO as N_{EO} increased from 8 to 34. $\Delta G(EO)/N_{EO}$, on the other hand, decreased with increasing N_{EO}; the $\Delta G(EO)/N_{EO}$ values of S1, S2, and S3 surfactants were 1.17, 0.56, and 0.30 kJ/mol EO, respectively. Thus, at 25 °C an EO unit was about 5 and 2 times more hydrophilic than a PO unit for S1 and S2, respectively; $\Delta G(EO)/N_{EO}$ and $\Delta G(PO)/N_{PO}$ are comparable for S3 with the longer PEO block. With increasing N_{EO}, more EO segments reside further away from the micelle core and well into the aqueous environment.[47] Thus, their hydration does not change much when micelles form and, hence, the reduction in $\Delta G(EO)/N_{EO}$ with increasing N_{EO} can be justified. Similar dependence of PEO block hydrophilicity was observed

TABLE 4: Different Free Energy Contributions for $C_iPO_nEO_j$ Micellization at 25 °C

	ΔG_{mic} (kJ/mol)	ΔG(C) (kJ/mol)	ΔG(EO+PO) (kJ/mol)	ΔG(EO) (kJ/mol)	ΔG(PO) (kJ/mol)	ΔG(EO)/N_{EO} (kJ/mol EO)	ΔG(PO)/N_{PO} (kJ/mol PO)	(ΔG(EO)/N_{EO})/ ΔG(PO)/N_{PO}
S1	−33.4	−45.6	12.2	9.35	2.85	1.168	0.234	4.99
S2	−32.3	−45.6	13.3	9.58	3.72	0.564	0.305	1.85
S3	−30.9	−45.6	14.7	10.03	4.40	0.295	0.361	0.87

TABLE 5: Parameters for Estimation of Free Energy of Micellization

	j	a_0[13] (Å^2)	a_h (Å^2)	l_c (Å)	l_{max} (Å)	δ (Å)	A_0[12,13]	A_1[12,13]	A_2[13]	v_t (Å^3)	σ_0[12] (erg/cm^2)	$\Delta G°$ at 25 °C (pred) (kJ/mol)
S1	10	21	44.4	16.1	16.7	2.434	6.839	−11.405	6.069	350.2	50	−33.5
S2	23	21	57.0	14.7	16.7	2.434	6.839	−11.405	6.069	350.2	50	−31.5
S3	46	21	70.2	12.2	16.7	2.434	6.839	−11.405	6.069	350.2	50	−29.0

for both C_iEO_j[10] and $EO_jPO_nEO_j$[29] types of amphiphiles, where it was found that as the PEO block length increased, its effectiveness per EO segment in increasing the cmc decreased.

We note that because of the manner in which we calculated the free energy contribution associated with EO, any positive free energy contribution associated with forming the micelle interface (unfavorable hydrocarbon − solvent contact) would be included in ΔG(EO). As a result, the ΔG(EO) values reported here may be larger than the actual free energy contribution associated with the PEO blocks; correspondingly, the actual free energy contribution associated with the PPO blocks could be larger than the ΔG(PO) values reported here.

Prediction of Free Energy of Micellization using Molecular Model. In the previous section, we used experimentally determined $\Delta G°$ for micellization of $C_iPO_nEO_j$ surfactants in order to establish the role of PPO. In this section, we utilize an analytical molecular model to predict the free energy of micellization of S1, S2, and S3. Molecular information for the surfactants of interest (rather than experimental results) is now the input for this model calculation.

Molecular thermodynamic theories, which incorporate the surfactant molecular architecture as well as solvent properties, have been developed for quantitative prediction of micellar solution properties for a range of surfactants.[11,12,14] Puvvada and Blankschtein predicted the free energy of micellization by adopting a conceptual thought process which involves the estimation of free energy change associated with the loss in conformational degrees of freedom due to alkyl chain localization at the micelle core, the free energy of mixing, and the free energy of interactions.[12] To make this theory easier to use, Naor et al.[13] approximated the free energy due to alkyl chain transfer at micelle core using a second-order polynomial, and derived the following analytical expression for the free energy of the micellization (Δg_{mic}) of C_iEO_j nonionic surfactants:

$$\Delta g_{mic} = kT\{[3.04 - 1.05(N_C - 1)](298\ K)T^{-1} - [5.06 + 0.44(N_C - 1)]\} + \sigma_0\left[1 - \frac{(S-1)\delta}{l_c}\right]\left[\frac{Sv_t}{l_c} - a_0\right] - kT\ln\left[1 - \left(\frac{a_h l_c}{Sv_t}\right)\right] + A_2(l_c/l_{max})^2 + A_1(l_c/l_{max}) + A_0 \quad (20)$$

where k is the Boltzmann constant, σ_0 the interfacial tension between bulk hydrocarbon and water, S the shape factor, δ the Tolman distance, v_t the volume of the hydrocarbon tail, a_0 the interfacial area screened from contact with water by the surfactant head, a_h the average cross-sectional area of the head, l_c the micelle core radius, l_{max} the hydrocarbon chain length when fully stretched, and N_C the number of carbon atoms in the alkyl chain, and A_0, A_1, and A_2 are constants.[13]

The molecular parameters used to estimate the free energy of micellization are listed in Table 5.

a_h: a_h for C_iEO_j surfactants can be approximated as[12,13]

$$a_h(T,j) = 38.1[1 - 0.0075(T - 298)](j/6)^n \quad (21)$$

Here n is 0.8 for N_{EO} up to 8, and n varies in the range of 0.3−0.5 for higher N_{EO}.[12] $n = 0.3$ was considered here to estimate a_h at 25 °C.

δ: δ can be estimated as[13] $\delta = 2.25 l_{max}/l_{max\ (N_C=12)}$ (in Å), where l_{max} is approximated as[13]

$$l_{max} = 1.54 + 1.265(N_C - 1) \quad (22)$$

v_t: v_t was estimated as[13]

$$v_t = 27.4 + 26.9(N_C - 1) \quad (23)$$

l_c: It was found that l_c varied with the alkyl chain length (N_C) but also with the hydrophilic segment length (N_{EO}). For the surfactants we consider here N_C is constant, but N_{EO} varies. The l_c values of $C_{12}EO_j$ surfactants (for $j = 4$, 6, and 8) were obtained from the literature[12] and extrapolated linearly to obtain the values that are applicable to S1, S2, and S3. We note that taking l_c as an independent input is an approximation in the molecular thermodynamic theory[12] wherein the free energy of micellization is minimized with respect to l_c, subject to the surfactant mass balance constraints.

In order to apply this molecular model to the case of $C_iPO_nEO_j$ surfactants, each PO unit is accounted for using its equivalent number of EO units (since PPO plays a hydrophilic role). From a comparison between ΔG(PO) and ΔG(EO), each PO unit is equivalent to 0.20, 0.54, and 1.1 EO units for S1, S2, and S3, respectively. Thus S1, S2, and S3 can be considered equivalent to $C_{13}EO_j$ surfactants with j being equal to 10, 23, and 46, respectively.

Free Energy of Micellization. The free energies of micellization at 25 °C predicted from eq 20 were −33.5, −31.5, and −29.0 kJ/mol for S1, S2, and S3, respectively. A very close agreement between thus calculated free energies and experimentally determined $\Delta G°$ has been achieved. The successful prediction of the free energy of micellization of $C_iPO_nEO_j$ surfactants using such a molecular model, with input parameters applicable to C_iEO_j surfactants and with the only adaptation from our side being the equivalence between PO and EO segments, reinforces the notion that PPO acts in a hydrophilic capacity during micellization, and suggests that the micellization of $C_iPO_nEO_j$ surfactants in aqueous solution is very similar to

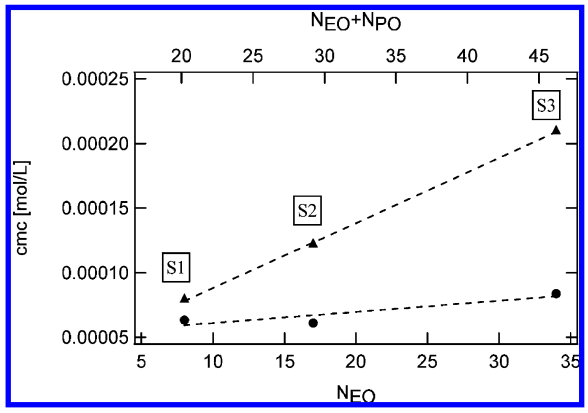

Figure 1. Influence of hydrophilic segment length on the critical micellization concentration of $C_iPO_nEO_j$ surfactants at (▲) 25 °C and (●) 40 °C. The cmc is plotted against the hydrophilic segment length expressed as N_{EO} (bottom x-axis) and ($N_{EO} + N_{PO}$) (top x-axis).

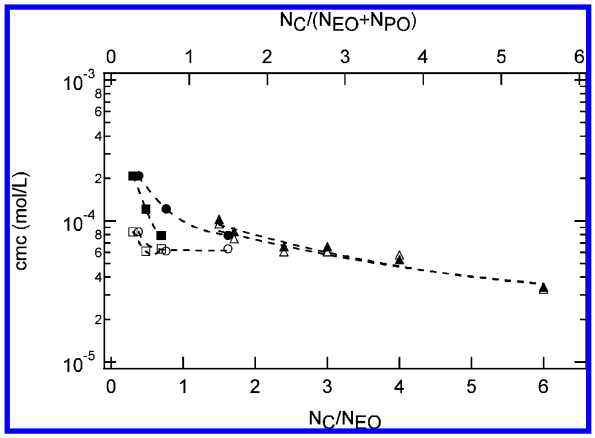

Figure 2. Comparison of critical micellization concentrations of $C_iPO_nEO_j$ surfactants with (▲) $C_{12}EO_j$ surfactants (cmc values obtained from ref 43). Filled symbols: 25 °C; empty symbols: 40 °C. $C_iPO_nEO_j$ cmcs are plotted against (●) N_C/N_{EO} and (■) $N_C/(N_{EO} + N_{PO})$.

that of C_iEO_j surfactants. Having validated the predictions of eq 20, one may now use this molecular model to predict $\Delta G°$ and cmc for $C_iPO_nEO_j$ surfactants of varying i, n, and j.

Influence of PEO in Micellization. An increase in the cmc values with PEO block length was found for the set of surfactants studied here (Table 2). The cmc values of S1, S2, and S3 in aqueous solution are plotted in Figure 1 as a function of the number of EO units (N_{EO}) (considering only PEO to be hydrophilic) and of the sum of EO and PO units ($N_{EO} + N_{PO}$) (taking both PEO and PPO hydrophilic). A linear dependency of cmc on N_{EO} and $N_{EO} + N_{PO}$ is observed.

The PEO contribution to $\Delta G°$ can be captured by the molecular theory[13] discussed above. The third term in eq 20 that accounts for the interfacial free energy when the hydrophilic part of the surfactant is placed at the interface[12] should not be affected by PEO chain length. The fourth term accounts for the free energy penalty due to steric repulsion which does depend on the headgroup size. A N_{EO} increase enhances such steric repulsion, and $\Delta G°$ become less negative.

Higher temperature favored micellization, resulting in lower cmc values and a decrease in the slope of the cmc vs N_{EO} and vs $N_{EO} + N_{PO}$ lines. This decreased surfactant hydrophilicity at higher temperature can be attributed to the dehydration of the hydrophilic parts. It is reported that temperature increase causes a dehydration of EO about 0.020 water molecules per °C.[12]

Comparison with C_iEO_j Surfactants. It is interesting to compare the micellization behavior of $C_iPO_nEO_j$ surfactants to that of the well-studied[43] alkyl ethoxylate (C_iEO_j) surfactants. The cmc values in aqueous solution for a series of $C_{12}EO_j$ surfactants[43] along with cmcs for $C_iPO_nEO_j$ are plotted in Figure 2 against the hydrophobic−hydrophilic segment length ratio (N_C/N_{EO}), since the N_C/N_{EO} composition has a major effect on the C_iEO_j micellization.[43] The cmc for both C_iEO_j and $C_iPO_nEO_j$ surfactants increased as the N_C/N_{EO} ratio decreased (and N_{EO} increased). It is observed from Figure 2 that the cmc of $C_iPO_nEO_j$ surfactants is more sensitive to the N_C/N_{EO} ratio (since the slope is higher) than the cmc of C_iEO_j surfactants. PPO is less hydrophilic than PEO; on the other hand, it is less hydrophobic than an alkyl chain. The enhanced sensitivity of $C_iPO_nEO_j$ cmc on N_C/N_{EO} can be attributed to the hydrophobicity induced due to the presence of PPO. The cmc for $C_iPO_nEO_j$ is plotted in Figure 2 also against $N_C/(N_{EO} + N_{PO})$. An even higher sensitivity of cmc on the surfactant composition ratio is observed under this consideration.

With increase in temperature, the cmc decreased for both C_iEO_j and $C_iPO_nEO_j$ types of surfactants. This cmc decrease was more pronounced for $C_iPO_nEO_j$ (as can be seen from Figure 2). It is also found that at 25 °C the cmc of $C_iPO_nEO_j$ seems to follow the same dependence on N_C/N_{EO} to that of C_iEO_j, but at 40 °C the cmc data do not follow the same line. This can be explained on the basis of higher degree of dehydration of PPO over PEO.[29]

We compare now the standard enthalpy and entropy of micellization of C_iEO_j and $C_iPO_nEO_j$ surfactants. We calculated $\Delta H°$ and $\Delta S°$ for C_iEO_j surfactants from the temperature variation of their cmcs using eqs 15−17. Both $\Delta H°$ and $\Delta S°$ are positive, indicating that the micellization of C_iEO_j surfactants is endothermic and entropy driven, similarly to the micellization of $C_iPO_nEO_j$ surfactants. $\Delta H°$ and $\Delta S°$ of micellization for both C_iEO_j and $C_iPO_nEO_j$ are found to vary linearly with N_C/N_{EO} and $N_C/(N_{EO} + N_{PO})$ (Figure 3). However, both ΔH and ΔS values are more composition sensitive (with higher slope) for the $C_iPO_nEO_j$ surfactants compared to C_iEO_j surfactants. The composition dependency of $\Delta H°$ and $\Delta S°$ for $C_iPO_nEO_j$ becomes stronger when both PEO and PPO blocks are considered as hydrophilic.

In order to decouple the influence of the hydrophilic headgroup from the overall chemical composition, $\Delta H°$ and $\Delta S°$ are normalized with N_{EO} for both types of amphiphiles and plotted in Figure 3 against N_C/N_{EO} and $N_C/(N_{EO} + N_{PO})$. Normalized $\Delta S°$ for both types of amphiphiles vary linearly with N_C/N_{EO}, exhibiting almost the same slope (a higher slope is obtained for $C_iPO_nEO_j$ surfactants when PPO is counted together with PEO). The positive dependence of $\Delta S°$ on N_C is consistent with the hydrophobic effect origin of $\Delta S°$. Normalized $\Delta H°$ values increase initially with increasing N_C/N_{EO} and $N_C/(N_{EO} + N_{PO})$, attain a maximum, and then start to decrease for both $C_iPO_nEO_j$ and C_iEO_j surfactants. This nonmonotonic dependence may reflect multiple (opposing) contributions to $\Delta H°$. Higher values of normalized $\Delta H°$ are observed for $C_iPO_nEO_j$ compared to C_iEO_j.

Comparison with $EO_jPO_nEO_j$ Block Copolymers. Extensive data are available in the literature for the self-assembly of $EO_jPO_nEO_j$ amphiphiles (Pluronics) in aqueous solutions.[29] The PEO and PPO blocks that are common in both $C_iPO_nEO_j$ and $EO_jPO_nEO_j$ types of amphiphiles motivate a comparison of their micellization behavior. Two homologous series of $EO_jPO_nEO_j$ amphiphiles, containing the same PPO block length, have been selected for this comparison. Their chemical composition, cmc values, and thermodynamic parameters are summarized in Table 6.[29] In order to compare the influence on micellization of

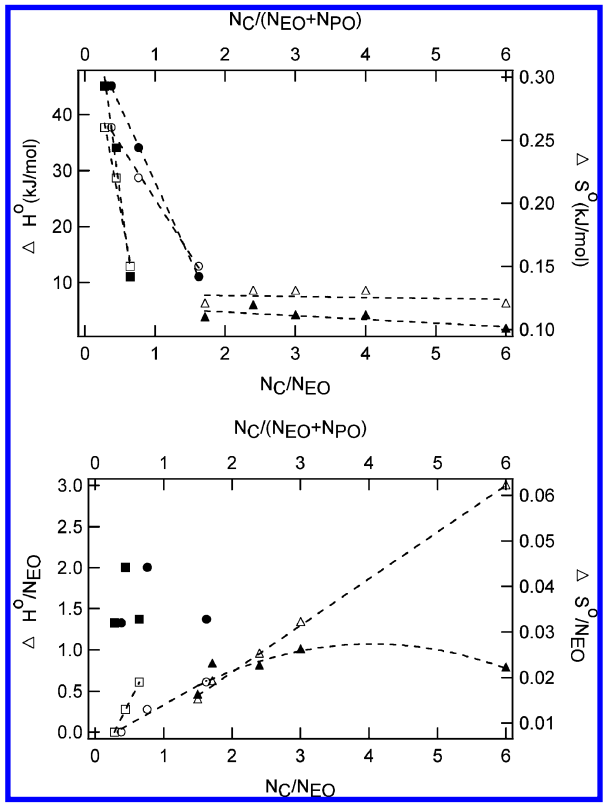

Figure 3. Comparison of standard enthalpies (filled symbols) and entropies (empty symbols) of micellization of $C_iPO_nEO_j$ in aqueous solutions with the corresponding values for (▲) $C_{12}EO_j$ surfactants (calculated using cmc values of ref 43). The standard enthalpy and entropy of $C_iPO_nEO_j$ are plotted against (●) N_C/N_{EO} and (■) $N_C/(N_{EO} + N_{PO})$.

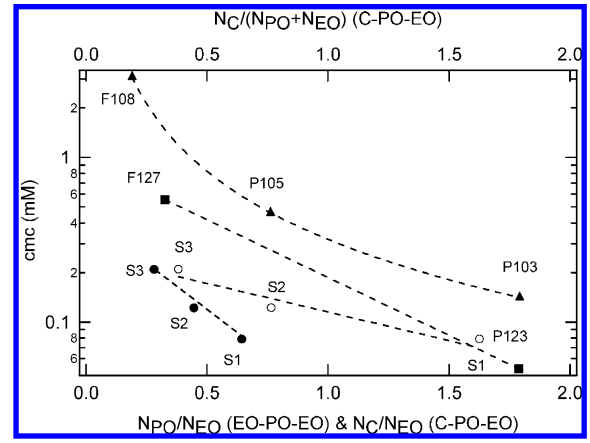

Figure 4. Comparison of critical micellization concentrations in aqueous solutions of $C_iPO_nEO_j$ and $EO_jPO_nEO_j$ (Pluronic) amphiphiles. The $EO_jPO_nEO_j$ cmcs are plotted against the N_{PO}/N_{EO} ratio and the cmcs of $C_iPO_nEO_j$ surfactants are plotted against (○) N_C/N_{EO} (bottom axis) and (●) $N_C/(N_{EO} + N_{PO})$ (top axis). (cmc values of $EO_jPO_nEO_j$ in aqueous solutions are obtained from ref 29).

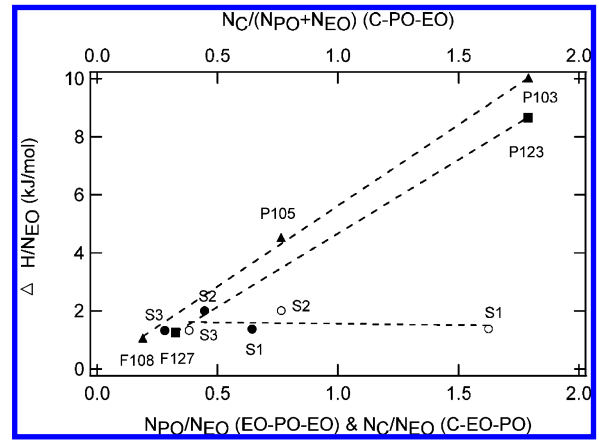

Figure 5. Comparison of the standard enthalpy of micellization in aqueous solutions of $C_iPO_nEO_j$ and $EO_jPO_nEO_j$ (Pluronic) amphiphiles. The standard enthalpies of EO−PO−EO per EO unit are plotted against the N_{PO}/N_{EO} ratio and the standard enthalpies of C−PO−EO per EO unit are plotted against (○) N_C/N_{EO} (bottom axis) and (●) $N_C/(N_{EO} + N_{PO})$ (top axis).

hydrophobic−hydrophilic composition, the cmc values of EO_jPO_n-EO_j and $C_iPO_nEO_j$ amphiphiles are plotted in Figure 4 against their composition (expressed as N_{PO}/N_{EO} for $EO_jPO_nEO_j$ and either N_C/N_{EO} or $N_C/(N_{EO} + N_{PO})$ for $C_iPO_nEO_j$). The cmcs of $C_iPO_nEO_j$ are lower than those of $EO_jPO_nEO_j$ due to the presence of the more hydrophobic alkyl chains in the former. The cmc and log(cmc) for both $EO_jPO_nEO_j$ and $C_iPO_nEO_j$ decrease monotonically with composition. For $C_iPO_nEO_j$, when the PPO block is considered together with the hydrophilic PEO, the log(cmcs) are found to be more sensitive (higher negative slope) to hydrophobic−hydrophilic composition ratio $N_C/(N_{EO} + N_{PO})$.

Enthalpies of micellization of $EO_jPO_nEO_j$ and $C_iPO_nEO_j$ (see Tables 3 and 6) are normalized with N_{EO} (so as to decouple the influence of PEO block size) and plotted against composition in Figure 5. The standard enthalpy of micellization per EO unit increased linearly as the hydrophobic−hydrophilic block length ratio increased in the case of $EO_jPO_nEO_j$ amphiphiles. In fact, the standard enthalpy per EO unit of $EO_jPO_nEO_j$ approached zero as the hydrophobic−hydrophilic block ratio approached zero, which indicates that the micellization process was dominated by the hydrophobic PPO block.[29] In comparison to the $\Delta H°/N_{EO}$ of $EO_jPO_nEO_j$, the $\Delta H°/N_{EO}$ of $C_iPO_nEO_j$ varies little with the hydrophobic−hydrophilic block length ratio.

$\Delta S°$ for both $EO_jPO_nEO_j$ and $C_iPO_nEO_j$ are positive (Tables 3 and 6). The standard entropy of micellization per EO unit is plotted in Figure 6 against composition for both types of amphiphiles. As the hydrophobic−hydrophilic block ratio increases, $\Delta S°/N_{EO}$ increases linearly for both types of amphiphiles. The effect of hydrophobic−hydrophilic block length ratio on $\Delta S°/N_{EO}$ appears weaker for $C_iPO_nEO_j$ in comparison to $EO_jPO_nEO_j$ amphiphiles when only the PEO part is considered to be hydrophilic, but stronger (steeper slope) when both PEO and PPO are considered as hydrophilic. We note that since the hydrophilicity of a PO unit is found equal or lower than that of a EO unit, the sum of $N_{EO} + N_{PO}$ is higher than the effective hydrophilic block length.

TABLE 6: Comparison with $EO_jPO_nEO_j$ Amphiphiles (Data from Ref 29)

Pluronic	MW	N_{PO}	N_{EO}	N_{PO}/N_{EO}	cmc (wt/vol)	cmc (mM)	$\Delta G°$ (kJ/mol)	$\Delta H°$ (kJ/mol)	$\Delta S°$ (kJ/(mol K))
P103	4950	60	2 × 17	1.791	0.07	0.141	−24.8	339	1.244
P105	6500	56	2 × 37	0.763	0.30	0.461	−25.6	331	1.212
F108	14600	50	2 × 132	0.190	4.50	3.082	−28.4	266	0.975
P123	5750	69	2 × 19	1.788	0.03	0.052	−24.9	329	1.223
F127	12600	65	2 × 100	0.326	0.70	0.555	−27.5	253	0.944

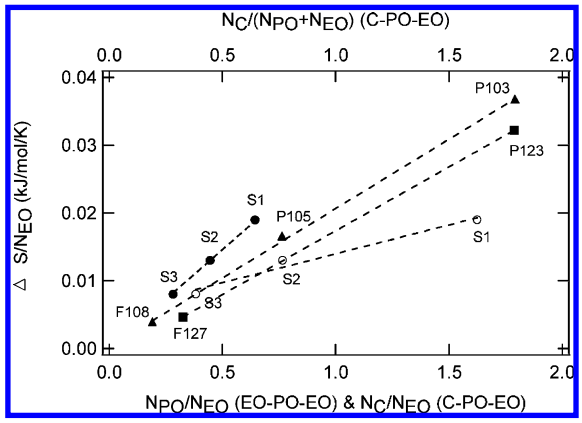

Figure 6. Comparison of standard entropy of micellization in aqueous solutions of $C_iPO_nEO_j$ and $EO_jPO_nEO_j$ (Pluronic) amphiphiles. The standard entropies of EO−PO−EO per EO unit are plotted against N_{PO}/N_{EO} and the standard entropies of C−PO−EO per EO unit are plotted against (○) N_C/N_{EO} (bottom axis) and (●) $N_C/(N_{EO} + N_{PO})$ (top axis).

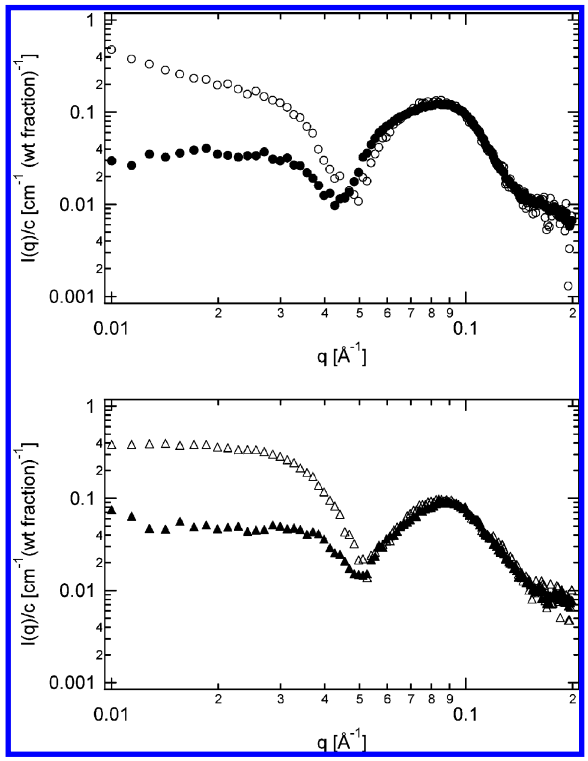

Figure 7. Reduced SAXS intensity data (in absolute scale) of (●) S2 and (▲) S3 normalized to unit concentration. Empty symbols: 5 wt % aqueous solution; Filled symbols: 15 wt % aqueous solution. The raw SAXS data had the water background subtracted and were corrected for beam stop shadowing, converted to absolute scale, and normalized with surfactant concentration.

In summary, the micellization of all three types of nonionic amphiphiles ($C_iPO_nEO_j$, C_iEO_j, and $EO_jPO_nEO_j$) is favored by higher temperature and disfavored by longer PEO block. The standard entropy per EO unit of micellization for all three surfactants is found to vary linearly with their hydrophobic−hydrophilic composition ratio. The composition dependence of $\Delta H°/N_{EO}$ is nonmonotonic for $C_iPO_nEO_j$ and C_iEO_j, different from the case of $EO_jPO_nEO_j$. Overall, the micellization of $C_iPO_nEO_j$ surfactants in aqueous solution resembles more that of C_iEO_j surfactants compared to $EO_jPO_nEO_j$.

Micelle Structure. The absolute scattering intensity data for two different surfactants at two concentrations, normalized with respect to the surfactant concentration, are plotted in Figure 7. The scattering curves appear similar for both S2 and S3. As the surfactant concentration increased from 5 to 15 wt %, the high q scattering intensity (related to the form factor) remained almost the same. Thus, we obtain an initial indication that the micelle shape and size remains approximately the same over the concentration range that we examined.[19] The decreased intensity in the low q range with increase in surfactant concentration is indicative of increasing interparticle interactions which can be accounted for by considering a suitable structure factor.[19]

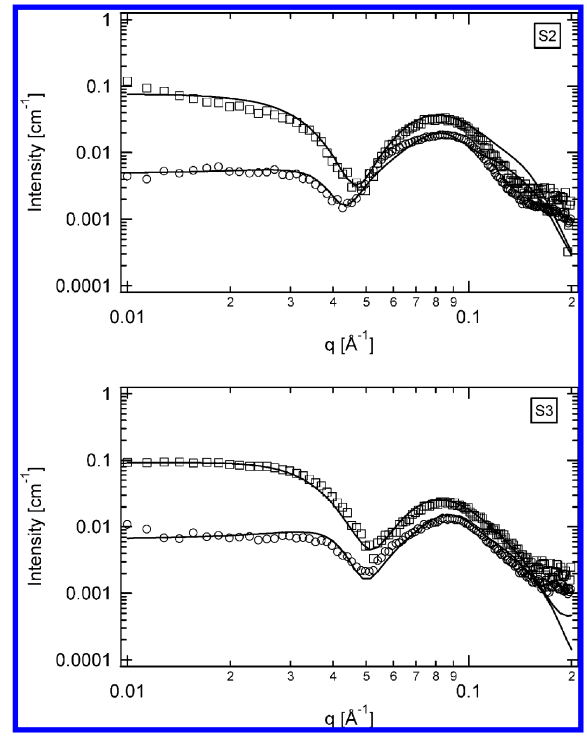

Figure 8. Reduced SAXS intensity data for (□) 5 and (○) 15 wt % aqueous solutions of S2 and S3 at 25 °C (the 5 wt % intensity data have been multiplied by a factor of 10). Solid lines represent fits to the core shell oblate ellipsoid. The fit parameters are presented in Table 8.

TABLE 7: Molecular Information Used for SAXS Data Analysis

material	chem formula	density (g cm^{-3})	vol per segment (cm^3)	$\rho = \sum(b/V)$ (Å^{-2})
PEO	$-(C_2H_4O)_n-$	1.114	65.6×10^{-24}	1.03×10^{-5}
PPO	$-(C_3H_6O)_n-$	1.0327	93.2×10^{-24}	9.69×10^{-6}
ethylene	$-(C_2H_4)_n-$	0.7564	46.5×10^{-24}	7.34×10^{-6}
water	H_2O	1.0	29.9×10^{-24}	9.46×10^{-6}

In order to extract micelle structure information from the scattering data, we considered several form factor models. Our criteria in selecting the best model have been the fit quality and how physically realistic the obtained parameters are. In one case, we assumed both alkyl and PPO to be present in the micelle core and PEO to be in the shell; however, no reasonable fit could be obtained under these constraints for spherical core−shell, oblate, or prolate ellipsoidal structures. In another case, we considered spherical micelles with three layers, having alkyl chains at the core, PPO at the middle layer, and PEO at the outer shell. Such three-layer model could only capture the scattering profile at lower q and failed at high q. We then assumed only alkyl chains to be present in the micelle core and all PPO and PEO to be present in the shell. Core−shell spheres did not provide a good fit, and fits to prolate ellipsoid resulted in micelle minor core radius that was unrealistic (greater than

TABLE 8: Micelle Structure Parameters Obtained from Fitting the Core Shell Oblate Ellipsoid Micellar Model for 5 and 15 wt % Aqueous Solutions of S2 and S3

surfactant	surfactant concn (wt %)	minor core radius (Å)	major core radius (Å)	minor shell radius (Å)	major shell radius (Å)	hard sphere radius (Å)	assocn no.	mol wt of micelle (kD)	solvation (vol %)	$N_{solvation}$
S2	5	15.0	38.0	43.0	70.0	80	259	425.0	56.7	5.0
S2	15	15.0	40.0	41.0	69.0	75	287	471.0	49.3	3.8
S3	5	15.0	33.0	44.5	72.0	80	195	466.1	56.0	4.7
S3	15	15.0	35.0	42.0	69.0	70	220	525.8	43.0	2.8

the extended length of alkyl chain). Finally, the core shell oblate (disk shaped) ellipsoid model provided a reasonable fit.

Scattering data with the core shell oblate ellipsoid model fits (solid lines) are presented in Figure 8. Structural parameters obtained from the fits for different systems are presented in Table 8. In these fits we assumed the micelle minor core radius equal to the extended alkyl chain length. The major core radius varies in the range 33−40 Å. The major core radius is found greater for S2 than S3. However, the micelle shell thickness of S3 is greater than that of S2 reflecting the longer PEO chain of S3. The major core radius increased for both S2 and S3 as the surfactant concentration increased from 5 to 15 wt %. Higher surfactant concentration resulted also in a decrease in the shell minor and major radii and an increase in the micelle association number. A similar increase has been obtained from neutron scattering for core−shell spherical micelles of the $C_{12}EO_{23}$ surfactant (Brij 35) in aqueous solution.[48] However, the micelle core radii (18−19 Å) obtained from this work[48] were higher than the fully stretched alkyl chain length.

The solvation ($\Phi_{solvation}$) of micelles is estimated using eqs 13 and 14 and the data presented in Table 8. The solvation is found in the range 43% to 57%. At 5 wt % surfactant concentration the % solvation is the same for both S2 and S3 micelles. The % solvation decreases with increase in surfactant concentration. $EO_jPO_nEO_j$ micelles in formamide showed a comparable degree of solvation of the PEO shell.[49] $N_{solvation,EO/PO}$ for S2 at 5 wt % solution is 5 and that for S3 at the same concentration is 4.7. At 15 wt % surfactant $N_{solvation,EO/PO}$ decreased to 3.8 for S2 and 2.8 for S3, as the micelles formed are more tightly packed. Similar solvation dependence on the amphiphile concentration has been reported for $EO_jPO_nEO_j$ micelles.[49]

It is valuable to compare the structure of S2 and S3 micelles with that of the well-studied[17−20,39] C_iEO_j micelles. An early suggestion of rodlike shape for C_iEO_j micelles was based on geometric consideration and minimal surface free energy calculation.[50] Intrinsic viscosity and sedimentation velocity experiments led Tanford et al. to propose the oblate ellipsoidal (disk shaped) shape to describe the $C_{12}EO_8$ (Brij 35) micelles in aqueous solution.[51] The $N_{solvation,EO}$ values obtained from their results ($N_{solvation,EO}$ = 3.3−2.7 for $C_{12}EO_8$, and $N_{solvation,EO}$ = 2.6 for $C_{12}EO_9$) are comparable with our results. Preu et al. proposed an ellipsoidal core shell model to describe the structure of $C_{12}EO_{23}$ (Brij 35) micelles.[17] The minor core radius obtained from their study was found in the range 15−17 Å which is comparable with our results. However, they reported a smaller major core radius compared to our result. Other groups described the structure of C_iEO_j micelles in aqueous solution using core−shell sphere form factor.[18−20] The influence of surfactant concentration on micelle structural parameters obtained from these studies is comparable with our results. The $C_{12}EO_{23}$ micelle structure in water was obtained by the generalized indirect Fourier transform (GIFT) method.[19] The micelle core radius varied within the fully stretched chain length of the alkyl chain. At higher surfactant concentration (above 10 wt %) an ellipsoidal (decaying rodlike) shape was found.[19] A recent neutron scattering study used an ellipsoidal model to capture the structure of $C_{14}EO_7$ and $C_{10}EO_7$ micelles.[39]

Conclusions

We report here on the micelles that a series of novel alkyl propoxy ethoxylate ($C_iPO_nEO_j$) surfactants with varying degree of ethoxylation form in water. To the best of our knowledge, this is the first experimental investigation of the micellization thermodynamics and micelle structure for such surfactants.

The micellization becomes more difficult as the poly(ethylene oxide) block length increases: the cmc doubled when the PEO length doubled. Higher temperature favors micellization: the cmc decreased by 20%, 50%, and 60% for $C_{13}(PO)_{12}(EO)_8$ (S1), $C_{13}(PO)_{12}(EO)_{17}$ (S2), and $C_{13}(PO)_{12}(EO)_{34}$ (S3), respectively, when the temperature increased from 25 to 40 °C.

The temperature dependence of the cmc and the corresponding free energy of micellization reveal a positive, unfavorable, enthalpy of micellization. A positive entropy contribution is the driving force for the $C_iPO_nEO_j$ micellization. An increase in the standard enthalpy and the entropy of micellization with N_{EO} has been observed.

The role of PPO is established by extracting its free energy contribution to micellization. ΔG(PO) does not favor the $C_iPO_nEO_j$ micellization. The hydrophilicity of a PO unit is comparable to that of an EO unit for S3, and lower than that of EO for S1 and S2, where an EO unit was found about 5 and 2 times, respectively, more hydrophilic than a PO unit.

The core shell oblate (disklike) ellipsoid model has been found to describe well the structure of S2 and S3 micelles in aqueous solution. As the PEO block length increases from S2 to S3, the shell radius increases and the micellar association number decreases. The micellar association number and micellar molecular weight increase little as the surfactant concentration increases. A higher degree of solvation is found for both S2 and S3 micelles at low surfactant concentration.

A close similarity between the micellization of aqueous solution of $C_iPO_nEO_j$ and C_iEO_j surfactants is found. However, the micellization of $C_iPO_nEO_j$ surfactants is more temperature sensitive due to the presence of the middle PPO block. For both types of surfactants $\Delta S°/N_{EO}$ varies linear with their hydrophobic−hydrophilic composition ratio. The composition dependence of $\Delta H°/N_{EO}$ is comparable for both types of surfactants, but stronger for $C_iPO_nEO_j$.

The micellization of $C_iPO_nEO_j$ surfactants in aqueous solution has also been compared with the micellization of $EO_jPO_nEO_j$ amphiphiles. PPO plays a different role (hydrophobic) in $EO_jPO_nEO_j$ compared to that in $C_iPO_nEO_j$ surfactants. A similarity is observed between the two types of surfactants on the influence of hydrophobic−hydrophilic composition ratio on the entropy of micellization per EO unit; however, $\Delta H°/N_{EO}$ is not comparable.

Acknowledgment. We thank Dr. S. Balijepalli and Dr. H. J. M. Gruenbauer of Dow Chemical Co. for providing the $C_iPO_nEO_j$ surfactants, and NSF (grant CBET-0421154) for funding the SAXS facility used in this work. We also thank Ms. Stephanie Lam, a UB undergraduate student, for assisting with fluorescence spectroscopy experiments.

References and Notes

(1) Alexandridis, P.; Lindman, B. *Amphiphilic block copolymers: self-assembly and applications*; Elsevier: Amsterdam, 2000.

(2) Sulthana, S. B.; Rao, P. V. C.; Bhat, S. G. T.; Nakano, T. Y.; Sugihara, G.; Rakshit, A. K. Solution properties of nonionic surfactants and their mixtures: Polyoxyethylene (10) alkyl ether [CnE10] and MEGA-10. *Langmuir* **2000**, *16*, 980–987.

(3) Rhein, L. D.; Schlossman, M.; O'Lenick, A.; Somasundaran, P. *Surfactants in personal care products and decorative cosmetics*, 3rd ed.; CRC Press: Boca Raton, FL, 2006; Vol. 135.

(4) Ameri, M.; Attwood, D.; Collett, J. H.; Booth, C. Self-assembly of alcohol ethoxylate non-ionic surfactants in aqueous solution. *J. Chem. Soc., Faraday Trans.* **1997**, *93* (15), 2545–2551.

(5) Aramaki, K.; Olsson, U.; Yamaguchi, Y.; Kunieda, H. Effect of water-soluble alcohols on surfactant aggregation in the C12CO8 system. *Langmuir* **1999**, *15*, 6226–6232.

(6) Becher, P.; Trifilet, S. Nonionic surface-active agents. 12. effect of solvent on thermodynamics of micellization. *J. Colloid Interface Sci.* **1973**, *43* (2), 485–490.

(7) Goto, A.; Takemoto, M.; Endo, F. A thermodynamic study on micellization of nonionic surfactant in water and in water-ethanol mixture by gel-filtration. *Bull. Chem. Soc. Jpn.* **1985**, *58* (1), 247–251.

(8) Mitchell, D. J.; Tiddy, G. J. T.; Waring, L.; Bostock, T.; McDonald, M. P. Phase-behavior of polyoxyethylene surfactants with water - mesophase structure and partial miscibility (cloud points). *J. Chem. Soc., Faraday Trans. 1* **1983**, *79*, 975–1000.

(9) Meguro, K.; Takasawa, Y.; Kawahashi, N.; Tabata, Y.; Ueno, M. Micellar properties of a series of octaethyleneglycol-n-alkyl ethers with homogeneous ethylene-oxide chain and their temperature-dependence. *J. Colloid Interface Sci.* **1981**, *83* (1), 50–56.

(10) Barry, B. W.; Eleini, D. I. D. Surface properties and micelle formation of long-chain polyoxyethylene nonionic surfactants. *J. Colloid Interface Sci.* **1976**, *54* (3), 339–347.

(11) Nagarajan, R.; Ruckenstein, E. Theory of surfactant self-assembly: A predictive molecular thermodynamic approach. *Langmuir* **1991**, *7*, 2934–2969.

(12) Puvvada, S.; Blankschtein, D. Molecular-thermodynamic approach to predict micellization, phase-behavior and phase-separation of micellar solutions.1. Application to nonionic surfactants. *J. Chem. Phys.* **1990**, *92* (6), 3710–3724.

(13) Naor, A.; Puvvada, S.; Blankschtein, D. An analytical expression for the free energy of micellization. *J. Phys. Chem.* **1992**, *96*, 7830–7832.

(14) Rao, I. V.; Ruckenstein, E. Micellization behavior in the presence of alcohols. *J. Colloid Interface Sci.* **1986**, *113* (2), 375–387.

(15) Rusdi, M.; Moroi, Y.; Hlaing, T.; Matsuoka, K. Micelle formation and surface adsorption of octaethylene glycol monoalkyl ether (CnE8). *Bull. Chem. Soc. Jpn.* **2005**, *78* (4), 604–610.

(16) Zhang, Z. Q.; Xu, G. Y.; Wang, F.; Du, G. Q. Aggregation behaviors and interfacial properties of oxyethylated nonionic surfactants. *J. Dispersion Sci. Technol.* **2005**, *26* (3), 297–302.

(17) Preu, H.; Zradba, A.; Rast, S.; Kunz, W.; Hardy, E. H.; Zeidler, M. D. Small angle neutron scattering of D2O-Brij 35 and D2O-alcohol-Brij 35 solutions and their modelling using the Percus-Yevick integral equation. *Phys. Chem. Chem. Phys.* **1999**, *1* (14), 3321–3329.

(18) Zulauf, M.; Weckstrom, K.; Hayter, J. B.; Degiorgio, V.; Corti, M. Neutron-scattering study of micelle structure in isotropic aqueous-solutions of poly(oxyethylene) amphiphiles. *J. Phys. Chem.* **1985**, *89*, 3411–3417.

(19) Tomsic, M.; Bester-Rogac, M.; Jamnik, A.; Kunz, W.; Touraud, D.; Bergmann, A.; Glatter, O. Nonionic surfactant Brij 35 in water and in various simple alcohols: Structural investigations by small-angle X-ray scattering and dynamic light scattering. *J. Phys. Chem. B* **2004**, *108*, 7021–7032.

(20) Schefer, J.; McDaniel, R.; Schoenborn, B. P. Small-angle neutron-scattering studies on Brij-58 micelles. *J. Phys. Chem.* **1988**, *92*, 729–732.

(21) Sommer, C.; Pedersen, J. S.; Garamus, V. M. Structure and interactions of block copolymer micelles of Brij 700 studied by combining small-angle X-ray and neutron scattering. *Langmuir* **2005**, *21*, 2137–2149.

(22) Tanford, C. *The hydrophobic effect: Formation of micelles and biological membranes*, 2nd ed; Wiley: New York, 1980.

(23) Hunter, R. J.; White, L. R. *Foundations of colloid science.* Clarendon Press, Oxford University Press: Oxford, UK, 1987.

(24) Bollmann, L.; Urade, V. N.; Hillhouse, H. W. Controlling interfacial curvature in nanoporous silica films formed by evaporation-induced self-assembly from nonionic surfactants. I. Evolution of nanoscale structures in coating solutions. *Langmuir* **2007**, *23*, 4257–4267.

(25) Ivanova, R.; Lindman, B.; Alexandridis, P. Effect of pharmaceutically acceptable glycols on the stability of the liquid crystalline gels formed by poloxamer 407 in water. *J. Colloid Interface Sci.* **2002**, *252* (1), 226–235.

(26) Svensson, B.; Olsson, U.; Alexandridis, P. Self-assembly of block copolymers in selective solvents: Influence of relative block size on phase behavior. *Langmuir* **2000**, *16*, 6839–6846.

(27) Yang, L.; Alexandridis, P. Polyoxyalkylene block copolymers in formamide-water mixed solvents: Micelle formation and structure studied by small-angle neutron scattering. *Langmuir* **2000**, *16*, 4819–4829.

(28) Zipfel, J.; Berghausen, J.; Schmidt, G.; Lindner, P.; Alexandridis, P.; Tsianou, M.; Richtering, W. Shear induced structures in lamellar phases of amphiphilic block copolymers. *Phys. Chem. Chem. Phys.* **1999**, *1*, 3905–3910.

(29) Alexandridis, P.; Holzwarth, J. F.; Hatton, T. A. Micellization of poly(ethylene oxide)-poly(proplene oxide)-poly(ethlene oxide) triblock copolymers in aqueous-solutions - thermodynamics of copolymer association. *Macromolecules* **1994**, *27*, 2414–2425.

(30) Holmqvist, P.; Alexandridis, P.; Lindman, B. Phase behavior and structure of ternary amphiphilic block copolymer-alkanol-water systems: Comparison of poly(ethylene oxide) poly(propylene oxide) to poly(ethylene oxide) poly(tetrahydrofuran) copolymers. *Langmuir* **1997**, *13*, 2471–2479.

(31) Kjellander, R.; Florin, E. Water structure and changes in thermal stability of the system poly(ethylene oxide)-water. *J. Chem. Soc., Faraday Trans. 1* **1981**, *77*, 2053–2077.

(32) Shusharina, N. P.; Alexandridis, P.; Linse, P.; Balijepalli, S.; Gruenbauer, H. J. M. Phase behavior and structure of an ABC triblock copolymer dissolved in selective solvent. *Eur. Phys. J. E* **2003**, *10* (1), 45–54.

(33) Shusharina, N. P.; Balijepalli, S.; Gruenbauer, H. J. M.; Alexandridis, P. Mean-field theory prediction of the phase behavior and phase structure of alkyl-propoxy-ethoxylate "graded" surfactants in water: Temperature and electrolyte effects. *Langmuir* **2003**, *19*, 4483–4492.

(34) Fustin, C. A.; Abetz, V.; Gohy, J. F. Triblock terpolymer micelles: A personal outlook. *Eur. Phys. J. E* **2005**, *16* (3), 291–302.

(35) Hadjichristidis, N.; Iatrou, H.; Pitsikalis, M.; Pispas, S.; Avgeropoulos, A. Linear and non-linear triblock terpolymers. Synthesis, self-assembly in selective solvents and in bulk. *Prog. Polym. Sci.* **2005**, *30* (7), 725–782.

(36) Nivaggioli, T.; Alexandridis, P.; Hatton, T. A.; Yekta, A.; Winnik, M. A. Fluorescence probe studies of Pluronic copolymer solutions as a function of temperature. *Langmuir* **1995**, *11*, 730–737.

(37) Lin, Y. N.; Alexandridis, P. Cosolvent effects on the micellization of an amphiphilic siloxane graft copolymer in aqueous solutions. *Langmuir* **2002**, *18*, 4220–4231.

(38) Pedersen, J. S. A flux- and background-optimized version of the NanoSTAR small-angle X-ray scattering camera for solution scattering. *J. Appl. Crystallogr.* **2004**, *37*, 369–380.

(39) Aldona, R. Small angle neutron scattering study of two nonionic surfactants in water micellar solutions. *Pramana—J. Phys.* **2008**, *71* (5), 1079–1083.

(40) Berr, S. S. Solvent isotope effects on alkyltrimethylammonium bromide micelles as a function of alkyl chain-length. *J. Phys. Chem.* **1987**, *91*, 4760–4765.

(41) Kotlarchyk, M.; Chen, S. H. Analysis of small-angle neutron-scattering spectra from polydisperse interacting colloids. *J. Chem. Phys.* **1983**, *79* (5), 2461–2469.

(42) Alexandridis, P.; Yang, L. SANS investigation of polyether block copolymer micelle structure in mixed solvents of water and formamide, ethanol, or glycerol. *Macromolecules* **2000**, *33* (15), 5574–5587.

(43) Rosen, M. J. *Surfactants and interfacial phenomena*, 3rd ed.; Wiley-Interscience: Hoboken, NJ, 2004.

(44) Rosen, M. J.; Cohen, A. W.; Dahanayake, M.; Hua, X. Y. Relationship of structure to properties in surfactants. 10. Surface and thermodynamics properties of 2-dodecyloxypoly(ethenoxyethanol)s, C12H25(OC2H4)XOH, in aqueous-solution. *J. Phys. Chem.* **1982**, *86*, 541–545.

(45) Evans, D. F.; Wennerström, H. *The Colloidal Domain: Where Physics, Chemistry, Biology, and Technology Meet*, 2nd ed.; Wiley-VCH: New York, 1999; pp xl, 632.

(46) Berthod, A.; Tomer, S.; Dorsey, J. G. Polyoxyethylene alkyl ether nonionic surfactants: physicochemical properties and use for cholesterol determination in food. *Talanta* **2001**, *55* (1), 69–83.

(47) Crook, E. H.; Trebbi, G. F.; Fordyce, D. B. Thermodynamic properties of solutions of homogeneous p,t-octylphenoxyethoxyethanols (OPE1−10). *J. Phys. Chem.* **1964**, *68*, 3592–3599.

(48) Borbely, S. Aggregate structure in aqueous solutions of Brij-35 nonionic surfactant studied by small-angle neutron scattering. *Langmuir* **2000**, *16*, 5540–5545.

(49) Alexandridis, P.; Yang, L. Micellization of polyoxyalkylene block copolymers in formamide. *Macromolecules* **2000**, *33* (9), 3382–3391.

(50) Becher, P. Nonionic surface-active compounds IV. Micelle formation by polyoxyethylene alkanols and alkyl phenols in aqueous solution. *J. Colloid Sci.* **1961**, *16* (1), 49–56.

(51) Tanford, C.; Nozaki, Y.; Rohde, M. F. Size and shape of globular micelles formed in aqueous-solution by n-alkyl polyoxyethylene ether. *J. Phys. Chem.* **1977**, *81*, 1555–1560.

JP910939Q